Angewandte Chemie
Eine Zeitschrift der Gesellschaft Deutscher Chemiker

Supporting Information

Beating Vesicles: Encapsulated Protein Oscillations Cause Dynamic Membrane Deformations

*Thomas Litschel, Beatrice Ramm, Roel Maas, Michael Heymann, and Petra Schwille**

anie_201808750_sm_miscellaneous_information.pdf
anie_201808750_sm_Video_S1.mp4
anie_201808750_sm_Video_S2.mp4
anie_201808750_sm_Video_S3.mp4
anie_201808750_sm_Video_S4.mp4
anie_201808750_sm_Video_S5.mp4
anie_201808750_sm_Video_S6.mp4
anie_201808750_sm_Video_S7.mp4
anie_201808750_sm_Video_S8.mp4

Supporting Information

Methods:

Proteins

The plasmids for the purification of His-MinD[1], His-EGFP-MinD[2] and His-MinE[1] have been described previously.

Purification of His-MinD, His-EGFP-MinD and His-MinE was performed essentially as described earlier[1]. For a detailed protocol see Ramm and Glock *et al*.[3] In brief, the His-tagged proteins were expressed in *E. coli* BL21 (DE3) and purified via Ni-NTA affinity purification. If needed, protein was further purified using gel filtration chromatography on a HiLoad 16/600 Superdex 200 prep-grade column (GE Healthcare, Chicago, USA) in storage buffer (50 mM HEPES, pH 7.25, 150 mM KCl, 10 % Glycerol, 0.1 mM EDTA) or buffer was exchanged to storage buffer using a gravity desalting column. Protein purity was assessed via SDS-PAGE and mass spectrometry. Proteins were quick frozen and stored in aliquots at -80°C until further use.

Inner and Outer Solution

All inner and outer solutions contain 25 mM tris-HCl (pH 7.5), 150 mM KCl and 5 mM $MgCl_2$ (i.e. 'Min protein reaction buffer' in previous publications).[1] In addition, the solution encapsulated in the GUVs contained 1.5 µM MinD, 1.4 µM eGFP-MinD, 3 µM MinE and 5 mM ATP. The chosen ATP concentration should in theory supply the reaction for several days; in practice, other factors limit the lifetime of the oscillations, for example, usually after 4-5 hours the proteins inside the GUVs start to aggregate.

As solvent we use deionized water (Merck Milli-Q®) with 15% iodixanol (from OptiPrep™, Sigma Aldrich). Iodixanol is used to increase the density of the encapsulated solution, in order to create a difference in density between the encapsulated solution and the GUV-surrounding solution, which is a necessary requirement for inverse emulsion methods for generating GUVs. Iodixanol allows for a high difference in density (which we found to increase vesicle yield) while not affecting the osmolarity of the solution considerably. The prepared solution has an osmolarity of 560 mOsm/kg (measure with Fiske® Micro-Osmometer Model 210).

As the GUV-surrounding solution we use the Min protein reaction buffer and adjust the osmolarity through different concentrations of glucose. For the experiments shown in Figure 1, 2 and S3 and Videos S1 – S5 we use 200 mM glucose to match the osmolarity of the inner solution (560 mOsm/kg). To obtain osmotically deflated GUVs (Figure 3, S4 and S5 and Videos S6 - S8) we use outer solution with 300 mM glucose, resulting in a higher osmolarity of 635 mOsm/kg, so that GUVs osmotically deflate while they are generated.

Lipids

We use DOPC (1,2-Dioleoyl-sn-glycero-3-phosphocholine, Avanti Polar Lipids, Inc.) and DOPG (1,2-Dioleoyl-sn-glycero-3-phosphoglycerol, Avanti Polar Lipids, Inc.) (both 25 mg/ml in chloroform) in a ratio of 4:1. A low fraction of the anionic DOPG lipids was chosen to improve vesicle yield. Vecchiarelli et al. investigated the effects of different DOPC:DOPG ratios and found that stable and long lived Min patterning dynamics can be observed within a certain range below and above the physiological ratio of uncharged to negatively charged lipids of 2:1.[5]

The preparation of the lipid-in-oil mixture is based on published protocols.[4] 77 µl of the lipid mix is given in a 10 ml glass vial and 600 µl chloroform is added. In experiments with labeled membranes, 3 µl DOPE-ATTO655 (0.1 mg/ml in chloroform) is added. While being mixed on a vortex mixer, 10 ml of a silicon oil (5 cSt) and mineral oil (Sigma-Aldrich, M5904) mix (4:1 ratio) is slowly added to the lipid solution. Since the lipids are not soluble in this mix of silicon oil, mineral oil and chloroform, the resulting liquid is cloudy.

Vesicle generation

Vesicles were produced using the cDICE method as described by Abkarian et al.[6] Instead of utilizing petri dishes as in the original protocol, we 3D printed the rotating chamber in which the vesicles are generated with a 3D printer (Formlabs Form 2, Clear Resin). Inner diameter of chamber: 7 cm, diameter top opening: 3 cm, height of chamber: 2 mm. A magnetic stirring device (outdated IKA-COMBIMAG RCH) served as a motor, after the heating unit was removed to expose the motor shaft.

The inner solution is loaded into a syringe (BD Luer-Lock™ 1-mL syringe) which is then placed into a syringe pump system (neMESYS base 120 with neMESYS 290N) and connected through tubing to a glass capillary (100 µm inner diameter). We use capillaries with a larger diameter than in the original publication, providing much less surface per volume for the Min proteins to bind to (although also resulting in GUVs that are more polydisperse).

700 µl of the outer solution is pipetted into the rotating chamber, followed by approximately 5 ml of the lipid-in-oil mixture. The capillary tip is then immersed in the oil phase and the inner phase injected at a flow rate of 50 µl/hr for 15 minutes. The vesicles are withdrawn from the cDICE chamber with a micropipette.

Imaging

The vesicles are pipetted into a microtiter plate for imaging (Greiner Bio-One, 96-well glass bottom SensoPlate™), which has been passivated beforehand with 50 µl of 5 mg/mL casein (Sigma Aldrich) for 20 minutes.

Imaging is then performed with an LSM 780/CC3 confocal microscope (Carl Zeiss, Germany) equipped with a C-Apochromat, 40x/1.2 W objective. We use PMT detectors (integration mode)

to detect fluorescence emission (excitation at 488 nm for eGFP and 633 nm for Atto655) and record confocal images.

All experiments were conducted at room temperature.

Data analysis

To create the kymographs in Figure 2, the GUVs were stabilized within each time series with Fiji's "Image Stabilizer" plugin and compensated for slight focus drifts (and thus a change in the diameter of the cross section of the GUV) by gradually scaling up the size of the GUV by a maximum of 2% over the course of the time series. The plots in Figure 2 (bottom row) were also generated with these stabilized time series. Video S1 shows the unedited time series of the experiments.

The z-stack time series in Videos S2 – S5 are created with Fiji's "3D Project" function without interpolating z-stack planes. The z-stack time series in Video S6, S7 and Figure 3F (perspective from a 90° "side view" angle) were created with the same tool, but with an activated interpolate function.

Supporting Figures:

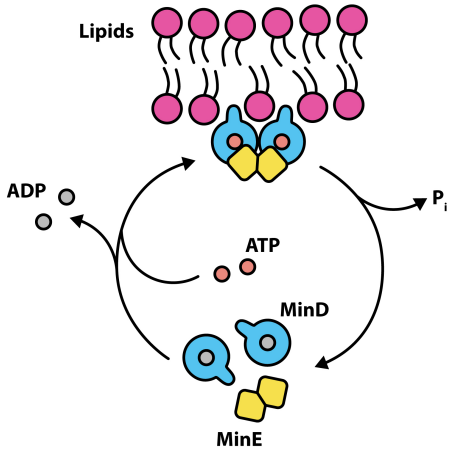

Figure S1. Min mechanism. Monomeric MinD binds ATP, which causes its dimerization and membrane binding. It then recruits further MinD-ATP (not shown here, but essential for pattern formation) and MinE, forming the membrane bound MinDE complex (top). MinE stimulates MinD's ATPase activity. ATP hydrolysis leads to the disintegration of the complex and detachment from the membrane. After detachment, monomeric MinD exchanges ADP for ATP before the cycle starts over again.

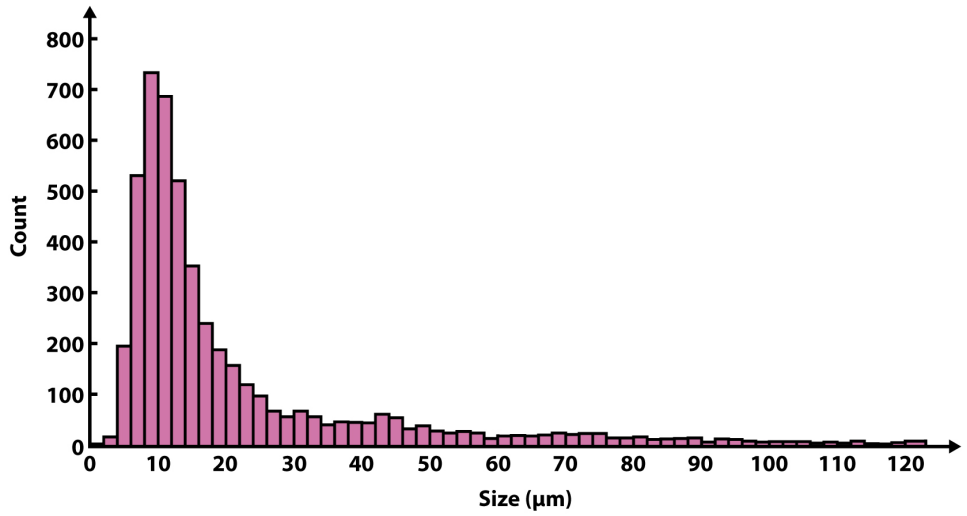

Figure S2. Size distribution of vesicles. The diameters of 4804 GUVs from 5 experiments were plotted in a histogram. Sizes were measured using DIC images with an overlaid fluorescent channel to confirm that the vesicles contain eGFP-MinD. The last bin on the right includes all vesicles with diameters of more than 120 µm.

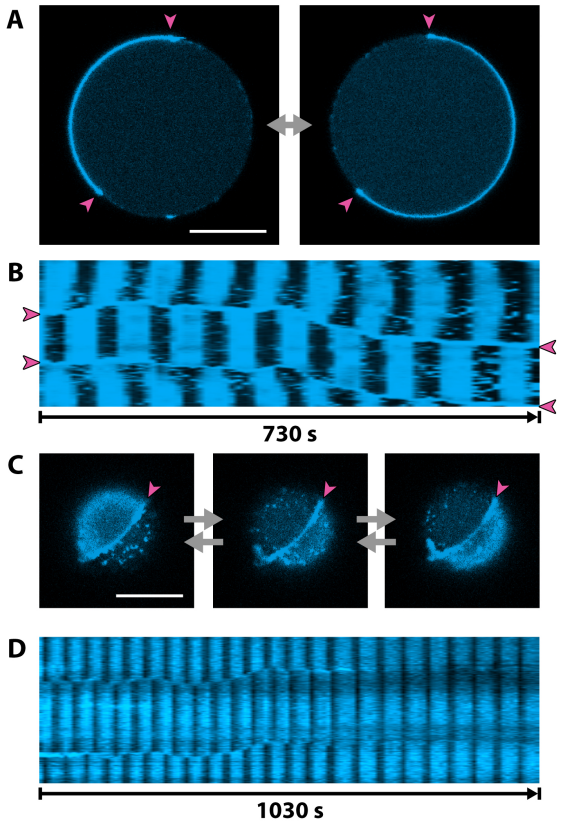

Figure S3. Second type of pole-to-pole oscillation. A) Confocal images of the equatorial plane. eGFP-MinD in cyan. B) Kymograph along the circumference of the GUV (equatorial plane). C) Confocal images of the GUV close to the glass surface. Magenta arrows in A) - C) highlight a ring-like structure made from MinD that spans once around the GUV and sets a boundary between the two oscillating poles of the GUV. Especially in C) the character of this ring is visible. Video S3 shows a time series of a 3D reconstruction of this vesicle. D) Kymograph along the circumference of a different GUV, showing a pole-to-pole oscillation of the second type, which then transition into a pulsing oscillation (see Figure 2 A-C). Scale bars are 10 µm.

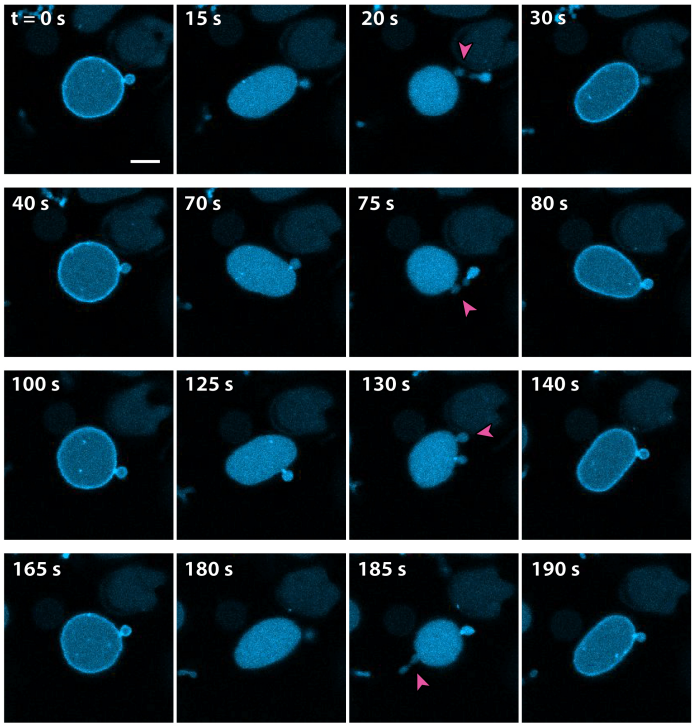

Figure S4. Sequential confocal images of a time series of a periodically budding vesicle. The vesicle undergoes a cycle of different shapes. Each row of images represents one cycle. In the first image in each row, the vesicle has an oblate-like shape (flattened), then changes to a prolate-like shape (elongated). After budding occurs, the shape of the vesicle becomes close to spherical. When the mother compartment merges with the vesicle bud, the vesicle takes on a prolate-like shape once more before the cycle starts over with an oblate-like shape. The vesicle buds are marked with magenta arrows. In the first two cycles the budding occurs at a position with a pre-existing bud, creating a chain of two buds (pearls). The scale bar in the first frame is 5 µm.

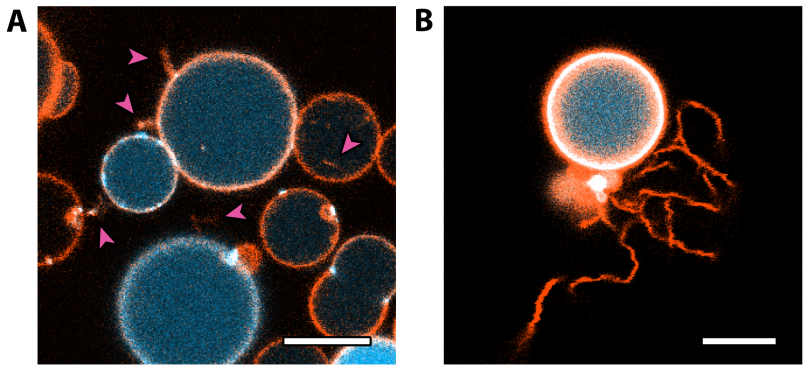

Figure S5. Membrane tubulation due to osmotic stress. A) Oscillating Min-containing GUVs (pulsing oscillation) with visible membrane tubules (purple arrows). When vesicles are generated with a difference in osmolarity between the inside and the outside phase, the resulting vesicles differ in morphology from simple spherical GUVs. Most vesicles respond with membrane tubulation, while only few assume vesicle shapes like in Figure 3. Through the formation of tubules, vesicles compensate for excess membrane (an increase in surface area to volume ratio) und hence can maintain a spherical shape. B) A single oscillating GUV generated under conditions with a high difference in osmolarity between inside and outside phase. Long membrane tubules can be seen. Scale bars are 10 µm.

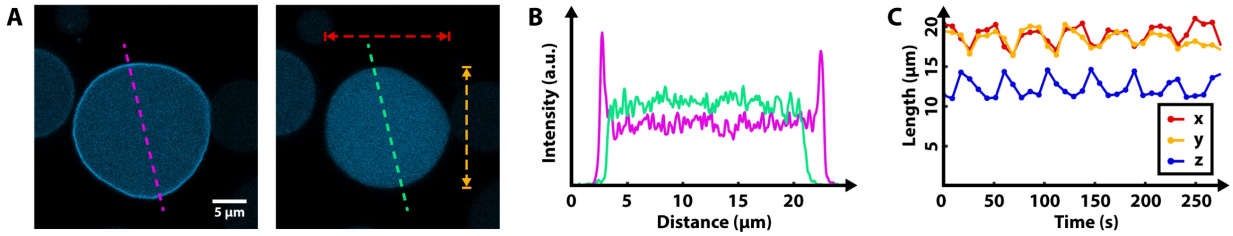

Figure S6. Analysis of the main compartment of periodically budding vesicle. Same vesicle as in Figure 3F. (A) Confocal sections of equatorial plane of GUV. In contrast to Figure 3D, which shows z-projections of confocal stacks, here only a single slice is shown, making the distribution of the protein clearer. Vesicle bud is not visible, because budding often occurs below the equatorial plane, closer to the glass surface. (B) Fluorescence intensity profile along purple and green dotted lines in (A). (C) Diameters of vesicle in y, x and z direction over time.

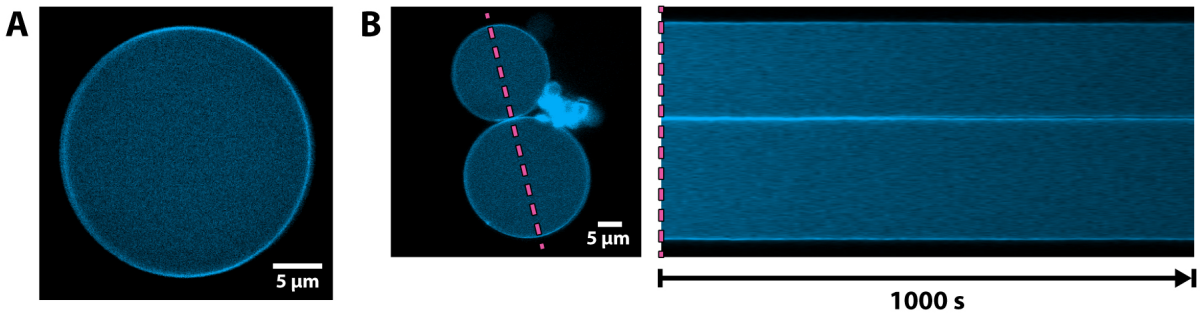

Figure S7. Control experiment without MinE. MinD-ATP binds to membrane, but cannot hydrolyze ATP due to the lack of MinE. MinD permanently binds to the membrane and no oscillations occur. (A) Single vesicle with membrane bound eGFP-MinD (cyan). (B) Image of two vesicles and kymograph along the dotted purple line. The kymograph shows no oscillations (only some photobleaching) over the course of 1000 s.

Supplementary References:

[1] M. Loose, E. Fischer-Friedrich, J. Ries, K. Kruse, P. Schwille, *Science* **2008**, *320*, 789-792.

[2] K. Zieske, J. Schweizer, P. Schwille, *FEBS Lett* **2014**, *588*, 2545-2549.

[3] B. Ramm, P. Glock, P. Schwille, *J Vis Exp* **2018**, e58139.

[4] a) C. Claudet, M. In, G. Massiera, *Eur Phys J E Soft Matter* **2016**, *39*, 9; b) E. Loiseau, J. A. Schneider, F. C. Keber, C. Pelzl, G. Massiera, G. Salbreux, A. R. Bausch, *Sci Adv* **2016**, *2*, e1500465.

[5] A. G. Vecchiarelli, M. Li, M. Mizuuchi, K. Mizuuchi, *Mol Microbiol* **2014**, *93*, 453-463.

[6] M. Abkarian, E. Loiseau, G. Massiera, *Soft Matter* **2011**, *7*, 4610-4614.